

PRIMAL: Processing-In-Memory based Low-Rank Adaptation for LLM Inference Accelerator

Yue Jiet Chong^{1†}, Yimin Wang^{2†}, Zhen Wu³, Xuanyao Fong⁴

Department of Electrical and Computer Engineering, National University of Singapore, Singapore

Email: {jason.yj.chong¹, kelvin.xy.fong⁴}@nus.edu.sg, {yimin.wang², e0323083³}@u.nus.edu

Abstract—This paper presents PRIMAL, a processing-in-memory (PIM) based large language model (LLM) inference accelerator with low-rank adaptation (LoRA). PRIMAL integrates heterogeneous PIM processing elements (PEs), interconnected by 2D-mesh inter-PE computational network (IPCN). A novel SRAM reprogramming and power gating (SRPG) scheme enables pipelined LoRA updates and sub-linear power scaling by overlapping reconfiguration with computation and gating idle resources. PRIMAL employs optimized spatial mapping and dataflow orchestration to minimize communication overhead, and achieves 1.5 \times throughput and 25 \times energy efficiency over NVIDIA H100 with LoRA rank 8 (Q,V) on Llama-13B.

Index Terms—Hardware-software co-design, low-rank adaptation (LoRA), processing-in-memory (PIM), LLM inference acceleration

I. INTRODUCTION

Recent advancements in LLMs have significantly enhanced their ability to perform complex tasks, leading to widespread adoption across various domains such as customer service, software engineering, and content generation [1]. Despite their general capabilities, models like GPT and LLaMA often fall short in meeting the specific requirements of downstream tasks, necessitating task-specific adaptation to improve performance and relevance [2]. Model adaptation enhances task alignment and offers a means to mitigate data privacy concerns by enabling on-premise or controlled fine-tuning. However, full model fine-tuning is computationally intensive and resource-demanding, making it impractical for many applications. To address this limitation, LoRA [3] has emerged as an efficient alternative.

LoRA introduces trainable low-rank matrices into specific layers of the transformer architecture without modifying the original model weights as shown in Fig. 1. For specific downstream tasks, only the low-rank matrices are substituted while the original model weights are retained. LoRA achieves performance comparable to full fine-tuning while significantly reducing computational and storage costs [3].

To exploit the benefits of LoRA and improve the energy efficiency and throughput for LLM inference, we studied

This work is funded in part by the National University of Singapore through the Microelectronics Seed Grant (FY2024); and in part by the National Research Foundation (NRF), Singapore, under the Competitive Research Programme (Award NRF-CRP24-2020-0002 and NRF-CRP24-2020-0003).

[†] Both authors contributed equally to this work.

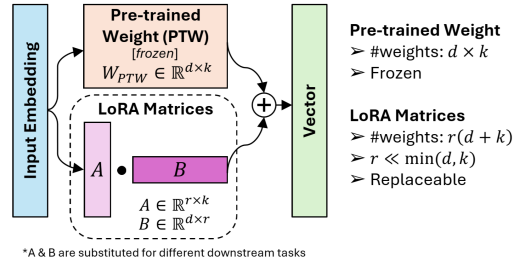


Fig. 1. The architecture of LoRA.

and implemented hardware-software co-design for LoRA integrated LLM inference accelerator, consisting of heterogeneous compute-in-memory PEs and IPCN.

II. PRIMAL HARDWARE ARCHITECTURE

The PRIMAL hardware architecture adopts a chiplet-based design, where each chiplet is referred to as a compute tile (CT). Each CT integrates a 2D-mesh IPCN that interconnects multiple heterogeneous PEs as shown in Fig. 2. The IPCN is responsible for dataflow control and executes dynamic data multiply-accumulate (DMAC) operations, representing $\mathbf{Q} \cdot \mathbf{K}^T$ of attention score. The PEs perform static weight multiply-accumulate (SMAC) operations, which correspond to matrix-vector multiplication in the Transformer [4] architecture.

A. Processing Element (PE)

The PE consists of a non-volatile resistive RAM analog compute-in-memory (RRAM-ACIM) macro and a volatile static RAM digital compute-in-memory (SRAM-DCIM) macro for SMAC of pre-trained weight matrices and LoRA matrices respectively.

1) *RRAM-ACIM*: The RRAM-ACIM macro [5] exhibits high density and non-volatility, making it particularly suitable for storing large, frozen pre-trained weight matrices. Its non-volatile nature allows the weights to be programmed only once for a base model, thereby significantly minimizing reconfiguration overhead. Once initialized, RRAM-ACIM performs SMAC operations directly in the analog domain, harnessing the inherent parallelism and energy efficiency of analog in-memory computing.

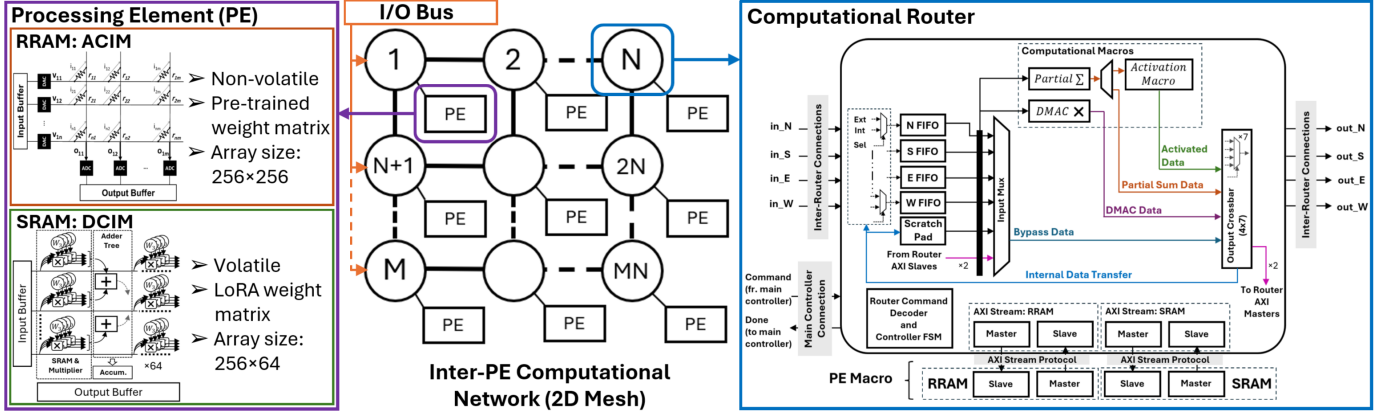


Fig. 2. Design of PRIMAL hardware (per compute tile): heterogeneous PE, 2D-Mesh IPCN, computational router.

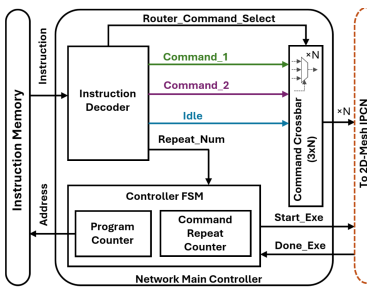


Fig. 3. The network main controller (NMC).

2) **SRAM-DCIM:** The SRAM-DCIM macro [6] offers fast write operations and highly accurate digital MAC operations, making it well-suited for accommodating LoRA matrices. Despite its lower density compared to RRAM-ACIM, this limitation is acceptable given the significantly reduced parameter count in LoRA. Moreover, the modular nature of LoRA, where matrices are frequently replaced to adapt to different downstream tasks, necessitates rapid reconfiguration. The fast programmability of SRAM enables efficient updates to LoRA weights, thereby minimizing operational stalls and enhancing system throughput and responsiveness.

B. Inter-PE Computational Network (IPCN)

The 2D-mesh IPCN is designed to facilitate seamless integration of compute-in-memory PE macros, enabling efficient orchestration of dataflow across the network to support diverse AI workloads. Computational tasks such as DMAC operations, partial sum accumulation, and activation operations are executed within the routers to enhance processing efficiency. To accommodate dynamic workload requirements, IPCN incorporates a dedicated instruction set architecture that enables re-programmable control over data movement and computation, ensuring adaptability and scalability.

The unit router features four planar ports dedicated to inter-router communication, along with two pairs of AXI-Stream adapters that interface with PEs with RRAM and SRAM, respectively. Each communication port incorporates

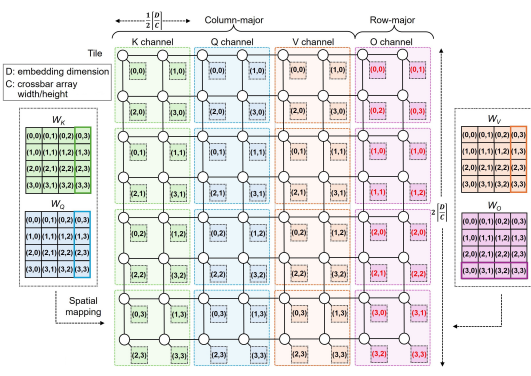


Fig. 4. The spatial mapping of weight matrices of an attention layer.

a FIFO buffer to facilitate temporary data storage and ensure smooth data flow. To support flexible data handling, the router enables internal data transfers between its buffers and macros. This capability allows efficient intra-router data movement, optimizing performance for various computational tasks. An integrated internal controller manages command reception and status reporting, enabling seamless coordination with the network main controller (NMC).

The NMC, shown in Fig. 3, governs data movement within the 2D-mesh IPCN and coordinates operation of the routers to establish dedicated dataflows optimized for specific LLM workloads, via a dedicated instruction set stored in the instruction memory. Due to operation redundancy in LLM workloads, each command to the routers is repeatable as governed by the controller via the instruction.

III. MAPPING AND DATAFLOW ORCHESTRATION

A. Mapping

The partitioned weight matrices W_Q , W_K , W_V , and W_O are spatially mapped onto the PE crossbar arrays, while the corresponding intermediate matrices Q , K , V , and O (query, key, value, and output, respectively) are allocated to distributed scratchpad memory. For weight placement on PE crossbars, each matrix is heuristically constrained to a column-wise

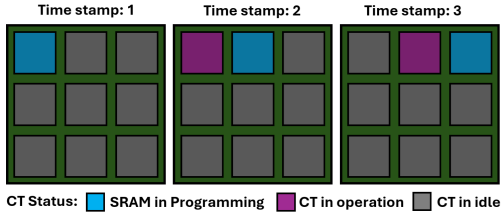


Fig. 5. Our Proposed SRAM Reprogramming and Power Gating (SRPG) scheme.

TABLE I
SYSTEM PARAMETERS

System Level			
Bit-width	64	Frequency	1 GHz
Compute Tile Level			
IPCN Dimension	32×32	PE #	1024
Macro Level (per unit Router-PE pair)			
RRAM-ACIM Array	256×256	SRAM-DCIM Array	256×64
Scratchpad Size	32 KB	FIFO Size (each)	128 B
DMAC #	16	I/O Pairs #	6

rectangular region (Fig. 4). The mapping process is optimized by tuning three key factors: intra-matrix shape, inter-matrix shape, and row–column ordering. Intermediate data are co-located with their associated weights to minimize communication overhead. Specifically, each intermediate matrix is stored in the scratchpad region corresponding to the PE array where its weight matrix resides. For example, \mathbf{Q} is placed in the scratchpads of the routers attaching to where \mathbf{W}_Q has been pre-mapped. This co-location strategy enables localized output reduction and improves data reuse efficiency.

Both pre-trained and LoRA weights adopt the same mapping strategy, as LoRA introduces low-rank adaptation matrices that are structurally aligned with the original weight matrices and hence, allows the same spatial partitioning and placement strategy to be applied without additional constraints.

B. Dataflow

The dataflow in LLM execution consists of three primary patterns: broadcast, reduction, and unicast. Initially, input embeddings are broadcast to the PE hosting \mathbf{W}_Q , \mathbf{W}_K , and \mathbf{W}_V for parallel computation. This enables parallel computation of the \mathbf{Q} , \mathbf{K} , and \mathbf{V} projections across multiple PEs. Since the weights are spatially distributed across multiple columns, a reduction phase aggregates the partial SMAC results from multiple PEs. Subsequently, unicast operations are employed to compute attention scores by performing $\mathbf{Q} \cdot \mathbf{K}^T$ using DMAC, followed by softmax activation. Unicast ensures that data is delivered point-to-point, reducing unnecessary traffic during the pairwise dot-product computation.

For key-value (KV) cache, during the decode phase, the \mathbf{K} and \mathbf{V} vectors associated with each generated token are appended to statically pre-allocated scratchpad buffers with pre-stored \mathbf{K}/\mathbf{V} during prefill. These buffers are organized in a cyclic fashion across distributed memory units, enabling uniform load distribution and mitigating memory contention.

TABLE II
PRIMAL BENCHMARKING: THROUGHPUT AND POWER

Model	LoRA* Matrices	Context Length (Input/Output)	Throughput (tokens/s)	Average Power (W)	Efficiency (tokens/J)
Llama 3.2 1B	Q	1024/1024	966.32	2.23	433.33
		2048/2048	565.46		253.57
	Q, V	1024/1024	963.47	9.58	432.04
		2048/2048	564.48		253.13
Llama 3 8B	Q	1024/1024	308.76	9.58	32.23
		2048/2048	221.37		23.11
	Q, V	1024/1024	307.89	14.76	32.12
		2048/2048	220.77		23.04
Llama 2 13B	Q	1024/1024	191.68	14.76	12.99
		2048/2048	145.81		9.88
	Q, V	1024/1024	190.98	14.76	12.94
		2048/2048	145.40		9.85

*LoRA with Rank 8

TABLE III
PRIMAL LATENCY: TTFT AND ITL

Model	LoRA* Matrices	Context Length (Input/Output)	TTFT (s)	ITL (ms)
Llama 3.2 1B	Q	1024/1024	0.370	1.708
		2048/2048	1.192	2.955
	Q, V	1024/1024	0.373	1.711
		2048/2048	1.199	2.958
Llama 3 8B	Q	1024/1024	0.710	5.726
		2048/2048	2.012	8.052
	Q, V	1024/1024	0.782	5.738
		2048/2048	2.037	8.065
Llama 2 13B	Q	1024/1024	0.962	9.494
		2048/2048	2.494	12.499
	Q, V	1024/1024	0.982	9.513
		2048/2048	2.533	12.518

*LoRA with Rank 8

The cyclic placement strategy ensures that scratchpad utilization remains balanced irrespective of sequence length, thereby sustaining throughput and minimizing latency in long-context inference scenarios.

The collective communication pattern is orchestrated using a spanning tree algorithm, which determines the routing paths for each phase. This algorithm ensures balanced and congestion-free traffic by leveraging the regular and aligned mapping of weights and intermediate data.

C. SRAM Reprogramming and Power Gating (SRPG)

For different downstream tasks, the LoRA matrices must be updated, which necessitates reprogramming the SRAM-DCIM macros. Additionally, LLM inference workloads are executed in a strictly sequential, layer-by-layer manner [7]. During the computation of a given layer, all other layers remain idle, presenting a significant opportunity for power optimization. To leverage both the sequential execution pattern and the SRAM reprogramming requirements, PRIMAL adopts a CT-based, layer-wise weight allocation strategy, which maps each layer to adjacent CTs.

As Fig. 5 shows, at the initialization phase for a distinct downstream task (Time Stamp 1), the SRAMs in the first CT are reprogrammed. Once the first CT begins executing its assigned workload, the SRAMs in the next CT are

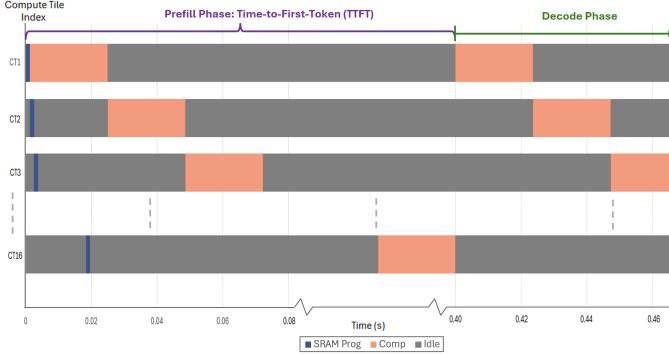


Fig. 6. The timing diagram of hardware scheduling for Llama 3.2-1B on PRIMAL.

reprogrammed in parallel. For CT in idle state, its IPCN and RRAM-ACIM macros are power-gated to save energy. However, the SRAMs and scratchpad memory macros remain powered on across all CTs to preserve volatile LoRA weights and ensure retention of context window data for KV caching, respectively. This operation scheme effectively reduces system power consumption by minimizing energy usage in idle CTs.

IV. SYSTEM EVALUATION

The system was evaluated through a comprehensive hardware-software co-verification methodology. Digital hardware components were designed and verified using Verilog HDL. Hardware synthesis was performed using *Synopsys Design Compiler*, followed by place-and-route using *Cadence Innovus*. Power and area of the scratchpad memory macro were obtained using *CACTI* [8], while other hardware macros were modeled and emulated in software using mathematical abstractions. Inference emulation and benchmarking were conducted using a cycle-accurate, instruction-level simulator based on the IPCN instruction set with the mapping scheme.

A. Performance Benchmarking

1) *Throughput and Power*: In PRIMAL, the average system power is dependent on the number of CTs. As the model size increases, the power consumption rises due to the activation of additional CTs required to store and process the expanded model weights. Concurrently, system throughput degrades as the enlarged model induces greater data movement and computational demands within the IPCN.

Compared to Nvidia H100, PRIMAL achieves $1.5\times$ throughput and $25\times$ energy efficiency (9.85 tks/J vs. 0.4 tks/J) for LoRA rank 8 (Q, V) on Llama-13B (2048/2048, Batch 1).

2) *Time-To-First-Token (TTFT)*: TTFT denotes the latency between the reception of a prompt and the generation of the first output token by the LLM. In PRIMAL, this corresponds to the prefill phase, which includes both the reprogramming of SRAM-DCIMs in the initial CT and the aggregate computation time across all LLM layers (Fig. 6). Due to pipelined execution scheme of PRIMAL, SRPG, the reprogramming of SRAM-DCIMs in subsequent CTs is effectively overlapped with computation and thus, does not contribute to TTFT.

TABLE IV
AVG. POWER & AREA BREAKDOWN OF HARDWARE MACROS (UNIT)

Macro	Power (uW)	Breakdown	Area (mm ²)	Breakdown
RRAM-ACIM [5]	120	9.9%	0.1442	65.2%
SRAM-DCIM [6]	950	78.1%	0.035	15.8%
Scratchpad Mem.	42	3.5%	0.013	5.9%
Router	103	8.5%	0.029	13.1%
Total (Router-PE pair)	1215	100%	0.2212	100%

Technology node: 7 nm; Area per CT Chiplet: 227.5 mm²

Consequently, TTFT is primarily bounded by the compute time of each CT, which serves as the critical path in the pipeline.

3) *Inter-token Latency (ITL)*: ITL, which corresponds to the decode phase, is primarily determined by the total number of layers in the LLM. As the model size scales, the number of layers increases proportionally, leading to deeper computational pipelines. Consequently, data must propagate through more layers that are mapped across additional CTs in PRIMAL, thereby incurring higher latency between successive token generations (Table III).

B. Hardware Scalability

The implementation of SRPG scheme enables power gating of IPCN and RRAM-ACIM macros within CTs in idle states, thereby substantially reducing overall system power consumption. Empirical evaluation on the various-size models demonstrates that SRPG achieves up to 80% power savings compared to the baseline configuration without power gating. Consequently, SRPG ensures that system power scales sub-linearly with respect to the LLM size (Table II), making PRIMAL highly scalable for running larger LLMs.

C. Macro Power and Area

The average power and area breakdown of the PRIMAL macros are summarized in Table IV. The RRAM-ACIM macro dominates area usage due to integrated analog SMAC operations and the need for DACs and ADCs. In contrast, the SRAM-DCIM macro, which performs digital SMAC using adder trees and shifters, eliminates converters and resulting in lower area but higher power consumption due to increased digital switching activity and less efficient digital computation.

V. CONCLUSION

Integrated with IPCN interconnect and adaptability of LoRA, PRIMAL leverages the energy efficiency of CIM to deliver energy efficient LLM inference while enabling seamless downstream task adaptation. Furthermore, the proposed SRPG mechanism ensures efficient SRAM reprogramming and optimizes the compute pipeline, achieving sub-linear power scaling with respect to LLM size. Evaluation shows it achieves $1.5\times$ throughput and $25\times$ energy efficiency improvement over Nvidia H100 for Llama-13B (2048/2048, LoRA rank 8 Q,V). Our design paradigm not only addresses the escalating energy demands of large-scale LLMs but also establishes PRIMAL as a highly scalable architecture, capable of supporting larger LLMs with LoRA at minimal power overhead via SRPG.

REFERENCES

- [1] Z. Chkirebene, R. Hamila, A. Gousssem, and U. Devrim, "Large language models (LLM) in industry: A survey of applications, challenges, and trends," in *2024 IEEE 21st International Conference on Smart Communities: Improving Quality of Life using AI, Robotics and IoT (HONET)*, 2024, pp. 229–234.
- [2] P. Kumar, "Large language models (llms): survey, technical frameworks, and future challenges," *Artificial Intelligence Review*, vol. 57, no. 10, p. 260, Aug 2024.
- [3] E. J. Hu, Y. Shen, P. Wallis, Z. Allen-Zhu, Y. Li, S. Wang, L. Wang, W. Chen *et al.*, "Lora: Low-rank adaptation of large language models." *ICLR*, vol. 1, no. 2, p. 3, 2022.
- [4] A. Vaswani, N. Shazeer, N. Parmar, J. Uszkoreit, L. Jones, A. N. Gomez, Ł. Kaiser, and I. Polosukhin, "Attention is all you need," *Advances in neural information processing systems*, vol. 30, 2017.
- [5] W. Wan, R. Kubendran, C. Schaefer, S. B. Eryilmaz, W. Zhang, D. Wu, S. Deiss, P. Raina, H. Qian, B. Gao *et al.*, "A compute-in-memory chip based on resistive random-access memory," *Nature*, vol. 608, no. 7923, pp. 504–512, 2022.
- [6] Y.-D. Chih, P.-H. Lee, H. Fujiwara, Y.-C. Shih, C.-F. Lee, R. Naous, Y.-L. Chen, C.-P. Lo, C.-H. Lu, H. Mori, W.-C. Zhao, D. Sun, M. E. Sinangil, Y.-H. Chen, T.-L. Chou, K. Akarvardar, H.-J. Liao, Y. Wang, M.-F. Chang, and T.-Y. J. Chang, "16.4 an 89tops/w and 16.3tops/mm² all-digital sram-based full-precision compute-in memory macro in 22nm for machine-learning edge applications," in *2021 IEEE International Solid-State Circuits Conference (ISSCC)*, vol. 64, 2021, pp. 252–254.
- [7] Y. Wang, Y. J. Chong, and X. Fong, "LEAP: LLM inference on scalable PIM-NoC architecture with balanced dataflow and fine-grained parallelism," in *2025 IEEE/ACM International Conference on Computer Aided Design (ICCAD)*, 2025, pp. 1–9.
- [8] N. Muralimanohar, R. Balasubramonian, and N. P. Jouppi, "Cacti 6.0: A tool to model large caches," *HP laboratories*, vol. 27, p. 28, 2009.